

# First-Principles Calculations of Hyperfine Parameters Using All-Electron Mixed-Basis Methods

著者	BAHRAMY Mohammad Saeed
号	51
学位授与番号	3818
URL	<a href="http://hdl.handle.net/10097/37486">http://hdl.handle.net/10097/37486</a>

	バハラミー	モハマド	サイード
氏名	BAHRAMY, Mohammad Saeed		
授与学位	博士(工学)		
学位授与年月日	平成19年3月27日		
学位授与の根拠法規	学位規則第4条第1項		
研究科, 専攻の名称	東北大学大学院工学研究科(博士課程) 知能デバイス材料学専攻		
学位論文題目	First-Principles Calculations of Hyperfine Parameters Using All-Electron Mixed-Basis Methods (全電子混合基底法による超微細構造定数の第一原理計算)		
指導教員	東北大学教授 川添 良幸		
論文審査委員	主査	東北大学教授 川添 良幸	東北大学教授 高梨 弘毅
		東北大学教授 粕谷 厚生	

## 論文内容要旨

The magnetic hyperfine interaction has attracted a great deal of attention since the early days of quantum mechanics. Experimentally, this interaction is probed through the spectroscopic techniques such electron paramagnetic resonance (EPR)[1] and nuclear magnetic resonance (NMR) [2]. These techniques are, in principle, very powerful tools for studying the atom-resolved contribution to the nuclear magnetic properties of complex systems, e.g. molecular radicals or point like defects in crystalline structures. However, the correct analysis of the experimentally observed hyperfine data is impeded by the lack of theoretical methods, which are sufficiently accurate and, furthermore, adequately efficient to perform the calculations in a reasonable time.

The aim of this thesis is to overcome the above difficulties by developing new computational methods, which are first and foremost accurate and, moreover, capable of performing the hyperfine calculations with the minimal computational effort. In this regard, within density functional theory (DFT), two accurate and efficient methods for calculating hyperfine parameters are presented, both based on the "all-electron" methods. In the former, the so-called "all-electron mixed-basis (AEMB) method" the one electron wavefunction is expanded in terms of both localized nucleus-centered atomic orbitals and plane waves and thereby affords an accurate representation for the spin density, of particular importance for hyperfine calculations, in the vicinity of nucleus as well as in the bonding regions. The current method is compared with the experiment and best computational methods reported in the literature. The mixed-basis approach is shown to yield highly accurate isotropic and anisotropic hyperfine parameters with modest computational effort. The atom-centered representation of the potentials and spin densities allows us to analyze, within the context of density functional theory, the effect of individual core levels in a physically transparent way

Inspired with the capabilities of the all-electron mixed-basis method, in the second approach we propose another alternative, a new method based on pseudopotential formalism. Within the second approach, so-called "all-electron pseudopotential (AEPP) method", the accurate hyperfine parameters can be efficiently achieved in a computationally even shorter time as compared to the first method, introduced above. The all-electron pseudopotential method is based on the evaluation of spin density at, and in the vicinity of, nucleus by reconstructing the all-electron wavefunctions from the corresponding pseudo-wave functions. For this purpose, first a transformation [3], so called "projector augmented wave (PAW)" is applied to reconstruct the frozen-core-all-electron wavefunctions in the core region. Second, the contributions of core orbitals to the charge density at the nucleus are evaluated by the means of first-order perturbation theory in which the perturbing potential is defined as a functional of charge and spin densities. Similar to the first method, the new method is applied to calculate the hyperfine parameters of various systems including the molecular complexes as well as the isolated Fe impurity doped in PdV alloys. Comparison with the experiment and the introduced all-electron mixed-basis method confirms the accuracy of the approach.

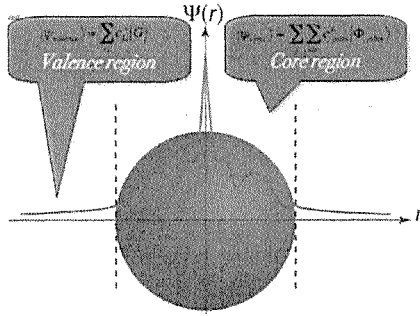


FIG 1. Schematic representation of all-electron mixed-basis method. The one-electron wavefunction is expanded in terms of both nucleus-centered wavefunctions within the core region and plane waves outside the atomic spheres.

In the AEMB formalism there are a number of parameters, which must be selected with care. Some parameters, such as the cutoff energy of the PW expansion of the potential are important for accurately computing the forces and thus affect the final geometry, but turn out to be rather unimportant for the hyperfine parameters (HFP's) when the correct geometry is used. Accurate forces were obtained with a potential cutoff energy of about 1000 eV for all elements considered with a single exception.

For hydrogen a higher value of 1500 to 2000 eV is required. Among the HFP's, it turns out that the isotropic (Fermi contact) HFP is far more sensitive to the choice of parameters than the anisotropic HFP's. Therefore, we shall focus on the effect of computational parameters on the Fermi contact-interaction. The atomic orbitals (AO's) used for expanding the one-electron Kohn-Sham wavefunctions are obtained from non-spin polarized atomic calculations. Generally, we select the ground state electronic occupation numbers for the atomic calculation. However, for ions we have found that more rapidly converging results are obtained if the AO's are derived from an atomic calculation with electronic occupation numbers that mimic the ion. Thus, for  $n$ -positive ions belonging to group II of the periodic table we selected a non-ground state electronic configuration with  $n$  outer  $s$  electron and  $n$  outer  $p$  ( $^{25}\text{Mg}^+$ ) or  $d$  ( $^{48}\text{Ca}^+$ ) electron. The outer  $p$  or  $d$  atomic orbital can be retained in the mixed-basis expansion for the wavefunctions but this has little effect on the computed HFP's. For the single atom and single ion calculations we selected a rather large atomic sphere size with a radius of 3 Å. Using this rather large size allowed optimal use of the AO's for the more extended outer  $s$  like states which benefits the accurate computation of the Fermi contact-interaction. Other important parameters are supercell size and plane wave (PW) cutoff energy for the expansion of the wavefunctions.

Figure 2-a indicates the convergence of the calculated Fermi contact-interaction of the  $^7\text{Li}$  atom with respect to supercell size. The cutoff energy for the PW expansion of the wavefunctions is 200 eV. A supercell size of 12 Å gives converged results that are in excellent agreement with experiment [4]. The supercell size plays an important role for atomic  $^7\text{Li}$  because of the spatial range of the  $2s$  wavefunction. For small supercells, the tails of the  $2s$  wavefunctions overlap with neighboring cells which in turn affects the  $1s$  wavefunction. For other atomic calculations the 12 Å has appeared sufficiently large also to assure convergence of the Fermi contact-interaction. Spatially extended clusters require larger supercell sizes, and a 12 Å separation distance is a guideline.

Figure 2-b shows the dependence of the Fermi contact-interaction of  $^7\text{Li}$  sample on the cutoff energy of the PW expansion of the wavefunctions. Clearly, the PW cutoff energy plays a minor role when compared to the supercell size. It appears that at a cutoff energy of 200 eV the wavefunctions are described with sufficient accuracy provided that the supercell is at least 12 Å. For large-scale calculations, where resources must be used most efficiently, it is likely that an even lower PW cutoff energy suffices.

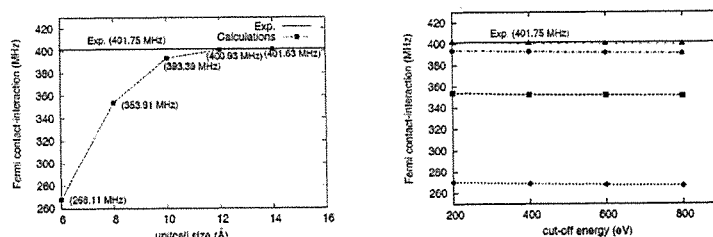


FIG 2. Computed Fermi contact interaction for atomic  $^7\text{Li}$  (a) as a function of supercell size, left picture and (b) as a function of the cut-off energy of the wavefunction plane wave expansion at supercell sizes of 6, 8, 10 and 12 Å (diamonds, squares, circles and triangles in the right panel). Lines are guide to the eye only. The experimental values (solid line) is from Ref. 4.

Figure 3 shows the radial representation of the spin density in real space in the vicinity of the nucleus

for different supercell sizes. The PW cutoff energy for the wavefunctions is 200 eV. The analytical data for atomic  ${}^7\text{Li}$  was calculated using the AtomDef Package with gradient-corrected exchange and Vosko-Wilk-Nusair correlation functionals. As could be expected from figure 2 the spin density near the nucleus is rather sensitive to the supercell size. The outer  $s$  like wavefunction, which is essential to properly describe the Fermi contact-interaction, is spatially very extended. Therefore, in reciprocal space there must be a dense grid around the  $\Gamma$  point. However, in these calculations on finite systems we do not perform  $k$ -point sampling ( $\Gamma$  point only). Thus, such a dense grid can be obtained only if the real space periodicity is sufficiently large. This also clarifies why the cutoff energy of the PW's for the wavefunction expansion is not so important, because this does not refine the grid. Rather as this energy is increased, more distant points are added to the grid.

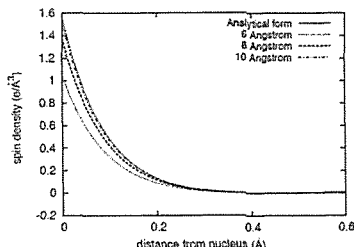


FIG 3. Computed radial spin density of atomic  ${}^7\text{Li}$  for various supercell sizes compared with analytic results (see text).

As mentioned, the AEMB has been applied to various structures including the molecular complexes and clusters. Here, we briefly discuss the AEMB results for zinc complexes and  $\text{Cu}_7$  cluster. In the former the effect of the electronegativity of X component on hyperfine properties of  $\text{ZnX}$  complexes has been studied. The chosen X elements in order of increasing electronegativity are:  $\text{Ag} < \text{H} < \text{CN} < \text{F}$ . Ag has about the same electronegativity as Zn. In the  $\text{ZnX}$  complexes a fully occupied bonding  $\sigma$  hybrid and a singly occupied antibonding  $\sigma$  hybrid exist between the  $\sigma$  molecular orbital (MO) of the X complex and the Zn  $4s$  atomic orbital (AO). Therefore, it is to be expected that with increasing electronegativity of X the bonding orbital becomes more like the  $\sigma$  AO (or MO) of X while the singly occupied molecular orbital (SOMO) becomes more like the Zn  $4s$  state. In other words, the spin becomes more localized on zinc and the Zn isotropic hyperfine interaction should increase. This trend is experimentally observed. In agreement with the experimental findings, our AEMB calculations confirm the presence of such a trend of spin distribution among  $\text{ZnX}$  complexes [5].

For the  $\text{Cu}_7$  calculations our calculations indicate that, the point group symmetry of the cluster is  $D_{5h}$ , a pentagonal bipyramid as illustrated in Figure 4 (left panel). The five copper atoms on the pentagonal ring are referred to as Cu(5), and the two axial copper atoms are labeled Cu(2).

AEMB computations reveals that the spin density is mostly on the Cu(2) atoms with minor contributions at the Cu(5) atoms as is evident from Figure 4 (right panel). Accordingly, the hyperfine parameters on the Cu(2) sites are dominant (1750 MHz for Fermi contact interaction). Anisotropy is absent on the Cu(5) sites which is in accordance with the assumption made in the related EPR experimental measurements [6]. The anisotropy on the Cu(2) sites is measured to be weak. The Cu(5) sites have negative HFP's. This negative sign indicates that the spin density near the Cu(5) nuclei is of opposite sign as the spin polarization of the  $\text{Cu}_7$  cluster. Relativistic effects turn out to be insignificant.

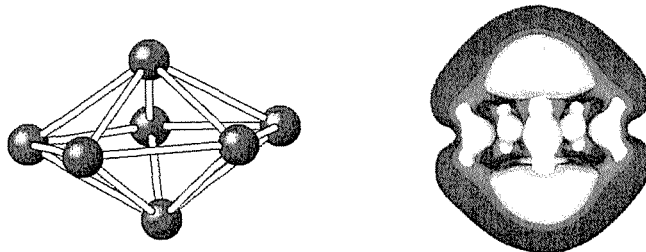


FIG 4. Bypiramid  $\text{Cu}_7$  structure (left) and its spin density distribution (right), isosurface coloration: white  $0.01\text{eV}/\text{\AA}^3$ , green  $0.0005\text{ eV}/\text{\AA}^3$ , and red  $0.0001\text{ eV}/\text{\AA}^3$ .

In the second part of the thesis, we have examined the accuracy of all-electron pseudopotential method by applying the approach to various structures. Also for the sake of completeness the obtained HFP's have been compared with the experiment and the other computational methods such as AEMB. As a first step to evaluate the accuracy of AEPP method, the feasibility of reconstructing all-electron (AE) wavefunctions from the corresponding pseudo-wavefunctions is examined. Figure 5 displays the

reconstructed using AEPP as well as the corresponding pseudo-wave obtained from a pseudopotential calculation. The figure clearly shows excellent agreement between the reconstructed  $2s$  orbital with the corresponding AEMB orbital. In fact the lines are essentially indistinguishable.

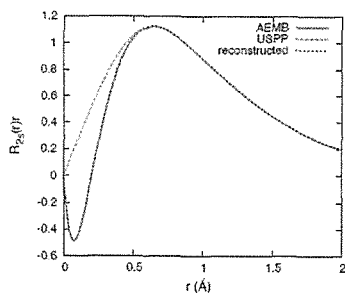


FIG 5. Radial part of  $2s$  orbital,  $R2s(r)$ , obtained directly from an all-electron mixed-basis calculation, AEMB (solid line), as obtained from reconstructing the pseudo wavefunctions (dotted line) and as obtained from corresponding ultrasoft pseudopotential calculation, USPP (dashed line).

To further test the accuracy of AEPP, it has been applied to calculate the contribution of core levels to the spin density at the nucleus,  $\rho_c(0)$ , of various elements, including a series of first-row elements and  $3d$ -transition metals, in their ground state electronic configurations. The calculated  $\rho_c(0)$  values along with the corresponding AEMB results have been listed in table 4.7 of thesis.

The table reveals that for first-row elements the reconstructed  $\rho_c(0)$  agree very well with the AEMB values. The difference between the two methods for this group of elements is less than 0.5%. For  $3d$ -transition metals also, in spite of the different character of the SOMO, a good agreement between reconstructed and directly calculated (with AEMB)  $\rho_c(0)$  values was obtained. The two methods differ most when the number of unpaired  $3d$ -electrons is largest. However, even in the extreme case of Mn, with the maximum number of unpaired electrons, this difference is still just 4.5%.

Interestingly, in both methods, the value of  $\rho_c(0)$  increases with the increase in the number of unpaired electrons. Accordingly, for Zn with fully occupied valence orbitals ( $3d^{10}4s^2$ ),  $\rho_c(0)$  becomes zero, whereas for Mn ( $3d^54s^2$ ), the absolute value of  $\rho_c(0)$  is the largest among the elements considered here.

Furthermore, it turns out that  $\rho_c(0)$  for elements with non- $s$ -like SOMO (e.g. F or Sc) is considerably larger than that for  $s$ -like SOMO (e.g. Cu). These are all in accordance with our earlier assumptions that the strength of induced core spin polarization depends sensitively on the number and type of unpaired electrons in SOMO's [5]. It is to be noted that  $\rho_c(0)$  is always negative. For the first-row elements it can be explained as follows: according to the Pauli exclusion principle, the exchange interaction induced by unpaired electrons is attractive but applicable to electrons in the same spin channel only [7]. As a result, the core  $1s$ -electrons of spin majority type are pulled a little outward thereby leaving behind a slight depletion of their corresponding charge density at the vicinity of nucleus. Thus, the spin density associated with core electrons becomes negative.

For  $3d$ -transition metals, a more complicated mechanism is needed for a proper interpretation of the negative sign of the core spin densities (see our discussion in section IV-B of Ref. 5).

In the thesis, a series of more complicated AEPP calculations have been presented for various molecular complexes including the radicals and transition metal complexes. Moreover, a detailed case study is devoted to investigate the role of vanadium on the formation and reduction of giant moments in PdV alloys doped by Fe impurity. For further information, the interested reader is referred to the thesis.

- [1] A. Abragam and B. Bleaney, *Electronic Paramagnetic Resonance of Transition Ions* (Clearendon Press, Oxford 1970).
- [2] I. Bertini, C. Luchinat, and G. Parigi, *Solution NMR of Paramagnetic molecules* (Elsevier, Amsterdam, 2001).
- [3] P. E. Blöchl, Phys. Rev. B **50**, 17953 (1994).
- [4] M. Filatov, and D. Cremer, J. Chem. Phys. **121**, 5618 (2004).
- [5] M. S. Bahramy, M. H. F. Sluiter, and Y. Kawazoe, Phys. Rev. B **73**, 045111 (2006).
- [6] R. Arratia-Perez, L. Alvarez-Thon, and F. Fuentealba, Chem. Phys. Lett. **397**, 408 (2004).
- [7] D. M. Chipman, Theor. Chim. Acta **82**, 93 (1992).

# 論文審査結果の要旨

本論文は、第一原理計算による超微細構造定数の詳細な算定に関する定式化、プログラム作成、超大規模シミュレーション計算実行を行い、実験値や従来の計算値との比較検討した結果をまとめたものである。超微細構造定数は、原子位置ごとの磁気モーメントの算定を可能とするため、実験的には、EPR（電子常磁性共鳴法）や NMR（核磁気共鳴法）によって盛んに研究されている。例えば、超微細構造定数は、分子中のラジカルの位置や結晶中の欠陥の位置の特定に極めて有効である。しかし、原子核位置での電子の波動関数を精密に求める必要があるため、従来の計算方法では極めて計算時間がかかる問題であり、実験を解析するに足るだけの高精度の計算は不可能であった。本研究では、全電子混合基底法及び全電子擬ポテンシャル法を活用することにより、この問題を抜本的に解決することに成功した。

第1章では、磁性研究の基盤の一つである超微細構造定数に関する歴史から現状の研究レベル全般までに関する概要を示す。従来からなされている実験的及び理論的研究の結果に対する検討を行い、それに基づき、本研究によるこれまでの問題点解決方法を述べる。

第2章では、本研究で活用する第一の計算方法である全電子混合基底法（AEMB）の定式化とプログラム上の詳細を述べる。AEMBは、系の波動関数を平面波と原子軌道の線形結合で表すことにより、少ない計算量で、原子間のみならず原子核周りの電子状態をも厳密に表現することが可能な優れた第一原理計算法の一つである。この結果、原子核位置の波動関数に敏感な超微細構造定数の等方的及び非等方的パラメータの両方の値を極めて高精度で算定することが可能となった。

第3章では、第2章の結果を基に、擬ポテンシャル法を活用した全電子擬ポテンシャル法（AEPP）による超微細構造定数計算の定式化を行っている。この計算方法は極めて高速に実行できるため、AEMBでは不可能な複雑な構造体や欠陥を含む結晶に対する数値計算をAEMBと同程度の計算精度で可能とした。原子核位置での波動関数は、PAW（Projector Augmented Wave）法により高精度で計算出来る。原子軌道からの原子核位置での寄与は摂動計算によって考慮している。

第4章では、先ず、AEMB及びAEPPの計算結果を実験値及び従来の計算結果と比較し、それらの妥当性を検討している。この章は2部から構成されている。最初の部分では、AEMBが種々の原子、イオン、分子、クラスターに対して適用され、比較検討がなされる。後半では、AEPPが超微細構造定数の実験値や計算値と比較され、評価される。最終的に、 $\text{Pd}_{0.95}\text{V}_{0.05}$ 中の希薄な鉄原子不純物に対する超大規模シミュレーション計算を実行し、巨大モーメントの生成消滅理由を明快に説明することに成功している。

第5章には、本論文の結論がまとめである。

以上、本研究は、超微細構造定数算定に対して独自の全電子混合基底法と全電子擬ポテンシャル法を開発し、詳細な第一原理計算を実行して従来法を遥かに超えた精度を達成すると共に、従来は不可能であった複雑な対象物に対する絶対値算定をも可能とし、新ナノ構造物質の重要な物性の算定法を確立したことにより材料工学の進歩に大いに寄与したと言える。

よって、本論文は博士(工学)の学位論文として合格と認める。